

**Analytical theoretical approach to the transient and steady state
voltammetric response of reaction mechanisms. Linear diffusion and
reaction layers at micro- and submicroelectrodes of arbitrary geometry**

Angela Molina^{*,a}, Joaquín González^a, Eduardo Laborda^a, Richard G. Compton^b

^a Departamento de Química Física, Facultad de Química, Regional Campus of International Excellence "Campus Mare Nostrum", Universidad de Murcia, 30100 Murcia, Spain

^b Department of Chemistry, Physical & Theoretical Chemistry Laboratory, Oxford University, South Parks Road, Oxford OX1 3QZ (UK). Fax: (+44) 1865-275-410

* Corresponding author:

Tel: +34 868 88 7524

Fax: +34 868 88 4148

Email: amolina@um.es

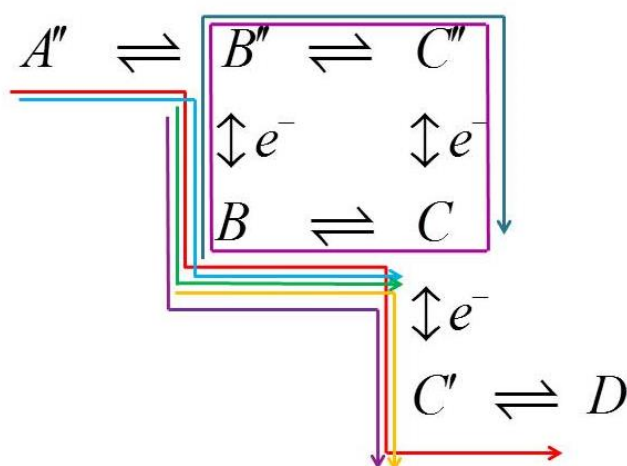
Abstract

A powerful theoretical approach to solve electrochemical reaction-diffusion problems with fast homogeneous kinetics is applied to obtain expressions for the transient current-potential-time response of a number of reaction mechanisms at microelectrodes of very different shapes, also applicable to ion transfer processes at liquid|liquid microinterfaces. The steady state response can be obtained as a limit when the characteristic dimension of the microelectrode tends to zero. Also, expressions under total chemical equilibrium conditions are derived when the linear reaction layer vanishes. The physico-chemical principles are based on suitable definitions of the so-called linear diffusion and reaction layers, which take into account the influence of the geometry of the diffusion field. The results presented fall within the so-called "kinetic steady state" and "diffusive-kinetic steady state" approaches and also give insight into the magnitude and extent of the perturbation of the chemical equilibrium conditions near the electrode surface as a consequence of the charge transfer process.

Keywords: Homogeneous chemical kinetics; Microelectrodes; Linear diffusion layer; Linear reaction layer; Transient current-potential response

1. Introduction

It is commonly found in electrochemical measurements that the electroactive species of the electrode process also take part in chemical reactions in solution, which alters their concentrations and so the electrochemical response [1–3]. Thus, let us consider the following reaction scheme with first-order homogeneous kinetics coupled to reversible electron transfers, which describes a great number of electrochemical processes:



Scheme I. Global reaction scheme under study. The arrows indicate different reaction paths: (red arrow) CECEC mechanism; (blue arrow) CEC mechanism; (green arrow) EC mechanism; (yellow arrow) CE mechanism; (purple arrow) ECE mechanism; (dark pink) Square Scheme (SQ); (dark green) open-Square Scheme (oSQ).

This general scheme includes quite a few simpler situations as particular cases:

CE mechanism



EC mechanism



ECE mechanism



CEC mechanism



Square scheme



open-Square scheme



CECEC mechanism



It is worth mentioning that the above reaction schemes can also be used to depict facilitated or inhibited ion transfer processes taking place at the interface between two immiscible electrolyte solutions (ITIES) via complexation (see for example [4,5]).

Another important reaction scheme that will be analyzed here is the catalytic mechanism where the product of the electrode reaction is regenerated in solution, in line with



An exact description of the voltammetric response of the above mechanisms is complicated as the electrode geometry plays a significant role, particularly at non-uniformly accessible interfaces as it is the case of microdiscs and microbands. In these situations, the derivation of a rigorous analytical solution is, in general, not possible. Moreover, numerical methods can get compromised or require sophisticated strategies for very fast chemical kinetics where very thin reaction layers are to be simulated [6]. Within this context, different approximate and semi-empirical treatments have been developed over years with the aim of obtaining manageable, explicit expressions for the steady state current-potential response of a particular reaction mechanism at a specific electrode geometry [7–12].

In this work, a more general, physically-sound and powerful analytical approach is proposed for solving any of the diffusion-reaction problems associated with mechanisms (1)-(8) whatever the electrode geometry. This is based on suitable definitions of the linear diffusion and reaction layers. From these definitions and making use of the so-called diffusive-kinetic steady state treatment (dkss), simple analytical expressions for the *transient* current-potential response are obtained. They enable accurate description of the influence of the chemical kinetics on the voltammetric and chronoamperometric response at microelectrodes of very different shapes. Also, the steady state and 'total equilibrium' responses are derived as limit cases where the characteristic dimension of the electrode tends to zero (or time goes to infinity) and the chemical kinetics is very fast, respectively.

2. Reaction mechanisms: a general theoretical approach to the problem

In all the above mechanisms, (pseudo-)first order homogeneous chemical reactions are coupled to reversible charge transfer steps. Hereafter, we will focus our approach on the chemical step common to all of them



that is characterized by the (pseudo)first-order rate constants, k_1 and k_2 , and by:

$$K = \frac{c_B^*}{c_C^*} = \frac{k_2}{k_1} \quad (10)$$

with c_B^* and c_C^* being the equilibrium concentrations such that the K -value corresponds to the inverse of the equilibrium constant.

Upon the application of a potential pulse E , the diffusive-kinetic differential equations of species B and C in reaction (9) for any electrode geometry are given by:

$$\begin{aligned} \frac{\partial c_B}{\partial t} &= D_B \nabla_G^2 c_B - k_1 c_B + k_2 c_C \\ \frac{\partial c_C}{\partial t} &= D_C \nabla_G^2 c_C + k_1 c_B - k_2 c_C \end{aligned} \quad (11)$$

where ∇_G^2 is the Laplacian operator for the electrode geometry G [13] and D_i is the diffusion coefficient of species i . Note that Eq. (11) is to be applied to species A'', B'', C'', C' and D' where appropriate.

The rigorous treatment of the influence of the chemical kinetics on the current-potential response for the above problems is, in general, very complex, especially in the case of non-uniformly accessible electrodes for which the Laplacian operator ∇_G^2 depends, besides on time, on more than one spatial coordinate; for example, in the case of disc microelectrodes, ∇_{disc}^2 depends on time (t) and on the radial (r) and normal (z) coordinates.

2.1. The kinetic steady state (kss) treatment: The linear reaction layers

The so-called kinetic steady-state (kss) approximation is a useful approach to address the above problem under transient conditions [2]. To introduce this treatment, it is convenient to define the following functions (see Eqs. (13)):

$$\begin{aligned}\zeta(q,t) &= c_B(q,t) + c_C(q,t) \\ \phi(q,t) &= c_B(q,t) - Kc_C(q,t)\end{aligned}\tag{12}$$

where q refers to *all* the spatial coordinate(s) corresponding to the electrode geometry considered. By inserting Eqs. (12) into (11) and assuming that the diffusion coefficients of species B and C are equal ($=D$), the following differential equations are obtained in terms of $\zeta(q,t)$ and $\phi(q,t)$,

$$\begin{aligned}\frac{\partial \zeta(q,t)}{\partial t} &= D \nabla_G^2 \zeta(q,t) \\ \frac{\partial \phi(q,t)}{\partial t} &= D \nabla_G^2 \phi(q,t) - \kappa \phi(q,t)\end{aligned}\tag{13}$$

where

$$\kappa = k_1 + k_2\tag{14}$$

Note that the above also holds for variables $\varsigma' (= c_{B'} + c_{C'})$ and $\phi' (= c_{B'} - Kc_{C'})$ and/or $\varsigma'' (= c_{B''} + c_{C''})$ and $\phi'' (= c_{B''} - Kc_{C''})$ when the reaction mechanism includes two or more chemical reactions (mechanisms (4)-(7)).

Apart from allowing for the simplification of the mathematical problem, it is important to consider the physicochemical meaning of variables $\varsigma(q,t)$ and $\phi(q,t)$. Thus, $\varsigma(q,t)$ corresponds to a pseudo-species with a concentration equivalent to the sum of concentrations of the species involved in the chemical process: B and C. Regarding $\phi(q,t)$, this is directly associated with the perturbation of the chemical equilibria B/C such that it takes a null value under equilibrium conditions ($\phi(q \rightarrow \infty, t) = 0$).

The kss approach only affects the pseudo-species ϕ and it consists in assuming that the perturbation of the chemical equilibrium is independent of time (*i.e.*, $\partial\phi/\partial t = 0$), which implies a stationary profile for ϕ . Thus, the validity of the kss approach corresponds to relatively fast chemical kinetics ($\kappa t > 5$) for any electrode size [14]. Under kss conditions the differential equation for ϕ becomes into

$$D\nabla_G^2\phi = \kappa\phi \quad (15)$$

with the boundary conditions for mechanisms (1)-(5) and (8) being given in Tables 1 and 2. For example, for spherical and hemispherical electrodes of radius r_s , the expression of ϕ obtained by solving the corresponding stationary differential equation (15) is [12]:

$$\phi(r) = \phi_s \frac{r_s}{r} e^{-\sqrt{\frac{\kappa}{D}}(r-r_s)} \quad (16)$$

with ϕ_s being the value of the pseudo-species ϕ at the electrode surface. Thus, the surface gradient of $\phi(r)$ is given by:

$$\left(\frac{\partial\phi}{\partial r}\right)_{r_s} = -\phi_s \left(\frac{1}{r_s} + \sqrt{\frac{\kappa}{D}}\right) \quad (17)$$

This can be viewed as the product of a function ϕ_s dependent on the surface conditions (that is, the applied potential and reaction mechanism) and a function dependent on the form of the Laplacian operator, the characteristic dimension of the microelectrode and the chemical kinetic rate constants. From the latter, a simple expression for the perturbed equilibrium zone, *i.e.* the thickness of the linear reaction layer at (hemi)spherical electrodes $\delta_{r,\text{sph}}$ can be immediately identified as the thickness corresponding to the linearised profile of the function ϕ (dashed lines in Figure 1) such that:

$$\left(\frac{\partial \phi}{\partial r}\right)_{r_s} = \frac{\phi_{\text{bulk}} - \phi_s}{\delta_{r,\text{sph}}} = \frac{-\phi_s}{\delta_{r,\text{sph}}} \rightarrow \delta_{r,\text{sph}} = \left(\frac{1}{r_s} + \sqrt{\frac{\kappa}{D}}\right)^{-1} \quad (18)$$

Note that, as discussed in reference [15], the mathematical form of ∇_G^2 does not depend on the surface conditions but on the electrode geometry G . Therefore, for a specific geometry, the thickness of the linear reaction layer is given by the same analytical equation whatever the mechanistic scheme, as shown in Figures 1 for the CE, EC and catalytic mechanisms at (hemi)spherical electrodes.

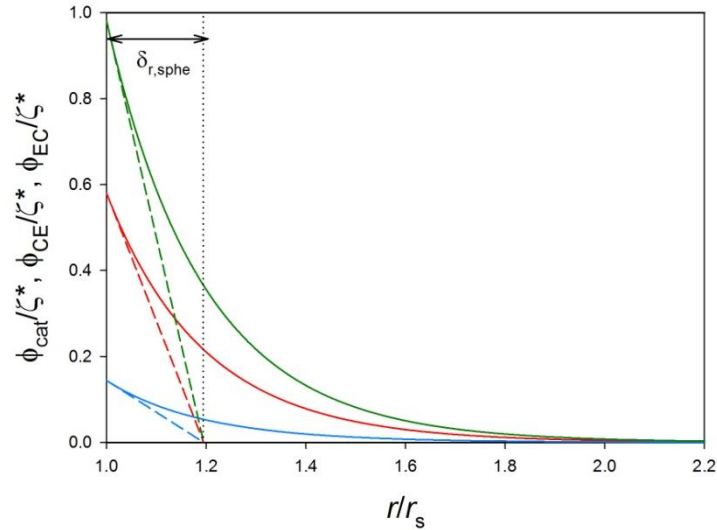


Figure 1. Kss profiles of the pseudo-species $\phi(r) = c_B(r) - Kc_C(r)$ corresponding to the catalytic (red line), CE (blue line) and EC (green line) mechanisms at a (hemi)spherical electrode calculated from Eqs. (16) and Eq. (10) in [16], Eqs. (B3) and (B4) in [17] and Eq. (A29) in [18], respectively. $\kappa = 100 \text{ s}^{-1}$, $K = 20$, $r_s = 10 \text{ }\mu\text{m}$, $D = 10^{-5} \text{ cm}^2 \text{ s}^{-1}$, $E - E^0 = -100 \text{ mV}$. $\zeta^* = c_B^* + c_C^*$

Once the expression for the pseudo-species $\phi(r)$ is known, that for $\zeta(r, t)$ must be determined from the combination of the differential equation (13) and the corresponding boundary conditions (Tables 1 and 2). For example, in the case of the CE mechanism at a spherical or hemispherical electrode of radius r_s the boundary conditions are given by [17]:

$$\left. \begin{array}{l} t = 0, r \geq r_s \\ t > 0, r \rightarrow \infty \end{array} \right\} \quad \left. \begin{array}{l} \zeta(r, t) = \zeta^* \\ c_D(r, t) = 0 \end{array} \right\} \quad (19)$$

$$t > 0, r = r_s \quad \left(\frac{\partial \zeta}{\partial r} \right)_{r=r_s} = - \left(\frac{\partial c_D}{\partial r} \right)_{r=r_s} \quad (20)$$

$$\left(\frac{\partial \zeta}{\partial r} \right)_{r=r_s} = \frac{1}{K} \frac{\phi_s}{\delta_{r, \text{sph}}} \quad (21)$$

$$\zeta_s - K \delta_{r, \text{sph}} \left(\frac{\partial \zeta}{\partial r} \right)_{r=r_s} = (1 + K) e^{\eta} c_{C', s} \quad (22)$$

where

$$\eta = \frac{F}{RT} (E - E^{0'}) \quad (23)$$

The resolution of the above problem upon the application of a potential pulse E leads to the following awkward expression for the current-potential-time kss response [17]:

$$I_{\text{CE, sph}}^{\text{kss}} = F A_s D \left(\frac{\partial \zeta}{\partial r} \right)_{r=r_s} = \frac{1}{K \delta_{r, \text{sph}} \Omega(E)} \left\{ 1 + \frac{2}{\sqrt{\pi}} (\Omega(E) - 1) \frac{F(\Theta(E))}{\Theta(E)} \right\} \quad (24)$$

with

$$\begin{aligned} \Omega(E) &= 1 + \frac{r_s}{K \delta_{r, \text{sph}}} (1 + (1 + K) e^{\eta}) \\ \Theta(E) &= \left(\frac{1 + K}{K} \right) (1 + e^{\eta}) \frac{2\sqrt{Dt}}{r_s} + (1 + (1 + K) e^{\eta}) \frac{2\sqrt{\kappa t}}{K} \\ F(x) &= \sqrt{\pi} \frac{x}{2} \exp\left(\frac{x}{2}\right)^2 \operatorname{erfc}\left(\frac{x}{2}\right) \end{aligned} \quad (25)$$

and $\operatorname{erfc}(x)$ being the complementary error function.

In the case of non-uniformly accessible electrodes (*i.e.*, microdiscs, microrings, microbands, ...), it has not been possible to complete a similar treatment due to the fact that, as

stated above, their theoretical study requires the use of two spatial coordinates and numerical simulation methods. For example, at disc electrodes, ϕ depends on r and z and $\phi_s = \phi(z=0, r)$. Nevertheless, the kss treatment does enable us to derive a suitable definition for the *average* thickness of the linear reaction layer. Hence, provided that the average surface flux of ϕ can be expressed, in analogy to Eq. (17), as the product of a function independent of the surface conditions and a potential-dependent function (ϕ_s) that takes an approximately uniform value across the electrode surface ($\approx \phi_s(E, \varpi, q_G)$, see Figure 6), then it follows that:

$$\left\langle \left(\frac{\partial \phi}{\partial q_N} \right) \right\rangle_{q_{N,s}} = \frac{-\phi_s(E, \varpi, q_G)}{\langle \delta_{r,G} \rangle} \rightarrow \langle \delta_{r,G} \rangle = \frac{-\phi_s(E, \varpi, q_G)}{\left\langle \left(\frac{\partial \phi}{\partial q_N} \right) \right\rangle_{q_{N,s}}} \quad (26)$$

where ϖ refers to the chemical (κ and/or K) and/or diffusive (D) parameters of the system, q_N is the coordinate normal to the electrode surface, $q_{N,s}$ is the q_N -value at the electrode surface and q_G is the characteristic dimension(s) of the electrode of geometry G.

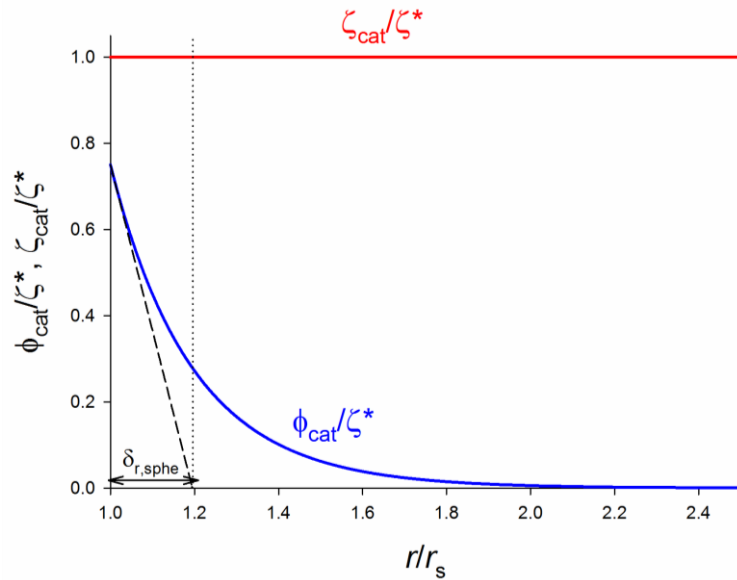


Figure 2. Profiles of the pseudo-species ϕ (blue line) and ζ (red line) corresponding to the catalytic mechanism under steady state conditions at a (hemi)spherical electrode calculated from Eq. (16) and Eq. (10) in [16]. $\zeta = c_B + c_C$, $\phi = c_B - Kc_C$. $\kappa = 100 \text{ s}^{-1}$, $K = 1$, $r_s = 10 \mu\text{m}$, $D = 10^{-5} \text{ cm}^2 \text{ s}^{-1}$, $E - E^{0'} = -50 \text{ mV}$. $\zeta^* = c_B^* + c_C^*$

By following the reasoning detailed in [15], the mathematical expression for $\langle \delta_{r,G} \rangle$ at a given microelectrode geometry can be obtained from the corresponding analytical solution for the current of the (pseudo)first-order catalytic mechanism. Indeed, in this particular case $\varsigma(q,t)$ is constant ($\varsigma(q,t) = c_B^* + c_C^* \quad \forall q,t$) (see Figure 2) and therefore the current response is only defined by the value of the surface gradient of variable ϕ , $\left(\frac{\partial \phi}{\partial q_N} \right)_{q_{N,S}}$ (see Tables 1-3). Hence, considering Eqs. (18) and (26) and given that ϕ_s is uniform (and constant) for any electrode geometry, only the linear reaction layer $\delta_{r,G}$ plays a role on the current. Thus, from the analytical solutions for the steady state limiting current of the catalytic mechanisms (reported for a variety of electrode geometries [19]), the corresponding expression for the average linear reaction layer can be easily extracted as indicated in Eq. (26) (see also [15], [19] and references therein). As discussed above, the $\langle \delta_{r,G} \rangle$ -value is dependent on the geometry of the diffusion field, as shown in Figure 3 where the linear reaction layer (identical for the catalytic, CE and EC mechanisms) at disc and ring microelectrodes are compared.

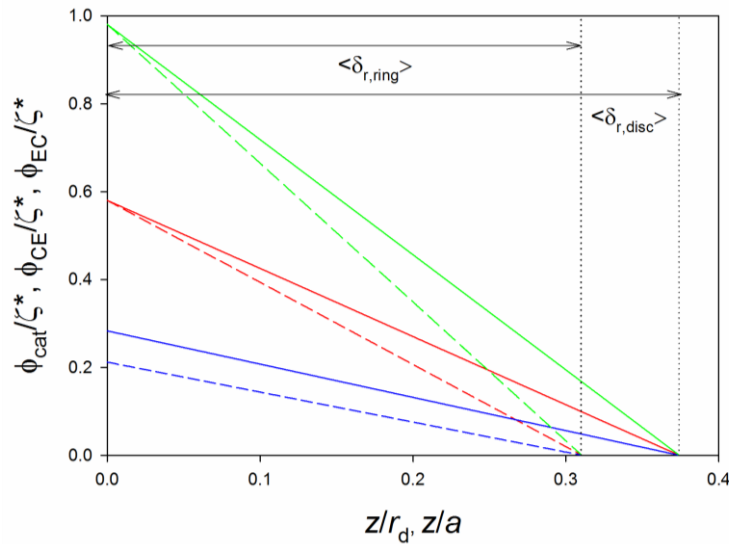


Figure 3. Linear profile for the pseudo-species $\phi/\varsigma^* = (\phi_s/\varsigma^*)(1 - z/\langle \delta_{r,G} \rangle)$ corresponding to the catalytic (red line), CE (blue line) and EC (green line) mechanisms at a disc ($r_d = 5 \mu m$, solid line) and a ring ($r_{outer} = a = 5 \mu m$ and $r_{inner} = 1 \mu m$, dashed line) electrodes calculated from the corresponding expressions in Table 3 and Eq. (10) in [16], Eqs. (B3) and (B4) in [17] and Eq. (A29)

in [18], respectively. $\phi = c_B - Kc_C$, $\zeta^* = c_B^* + c_C^*$. $\kappa = 100 \text{ s}^{-1}$, $K = 20$, $D = 10^{-5} \text{ cm}^2 \text{ s}^{-1}$, $E - E^0 = -100 \text{ mV}$. $\zeta^* = c_B^* + c_C^*$

2.2. The diffusive-kinetic steady state (dkss) treatment: The transient linear diffusion layers

The kss approximation simplifies the problem by supposing an stationary behaviour for the pseudo-species $\phi(q)$, which enables us to establish suitable definitions for the linear reaction layers. Nevertheless, finding expressions for $\zeta(q,t)$, the linear diffusion layer δ [20] and the current response for a given reaction mechanism can be cumbersome or even impossible in the case of non-uniformly accessible electrodes. Thus, additional assumptions can be introduced to further simplify the resolution of the reaction-diffusion problem of a given reaction mechanism. In the so-called diffusive-kinetic steady-state (dkss) treatment [12,17] this is done by considering that $\zeta(q,t)$ has a mathematical form analogous to that of a species only subject to diffusion transport that in the case of (hemi)spherical electrodes is given by:

$$\zeta(r,t) = \zeta^* - \frac{r_s}{r} (\zeta^* - \zeta_s) \operatorname{erfc} \left(\frac{r - r_s}{2\sqrt{Dt}} \right) \quad (27)$$

and, in general, for any electrode geometry by:

$$\zeta(q,t) = \zeta^* + [\langle \zeta_s \rangle - \zeta^*] F_G(q_G, q, t) \quad (28)$$

where $\langle \zeta_s \rangle$ refers to the average value of function $\zeta(q,t)$ at the electrode surface and

$F_G(q_G, q, t)$ is a function the expression of which depends on the particular electrode geometry.

The above dkss assumptions have been found to lead to accurate results at microelectrodes of typical sizes ($r_0 \leq \sqrt{Dt}$; for example, $r_0 \leq 30 \mu\text{m}$ for $t = 1 \text{ s}$ and $D = 10^{-5} \text{ cm}^2 \text{ s}^{-1}$) [21] (and also at macroelectrodes when the chemical kinetics is very fast ($\kappa \gg 1$) [14]). Therefore, the expressions reported in Table 5 can be used for quantitative characterization of homogeneous chemical kinetics from experimental voltammetric or chronoamperometric measurements.

From Eq. (27) the time-dependent linear diffusion layer at (hemi)spherical electrodes can be immediately obtained from:

$$\left(\frac{\partial \zeta}{\partial r}\right)_{r_s} = \frac{\zeta^* - \zeta_s}{\delta_{\text{sph}}} \rightarrow \delta_{\text{sph}} = \left(\frac{1}{r_s} + \frac{1}{\sqrt{\pi D t}}\right)^{-1} \quad (29)$$

At non-uniformly accessible electrodes, it can be assumed that ζ_s takes a uniform value across the electrode surface ($\langle \zeta_s \rangle = \zeta_s(E, \varpi, q_G, t)$) such that the average surface flux of ζ is given by:

$$\left\langle \left(\frac{\partial \zeta}{\partial q_N} \right) \right\rangle_{q_{N,S}} = \frac{\zeta^* - \zeta_s(E, \varpi, q_G, t)}{\langle \delta(q_G, t) \rangle} \quad (30)$$

where $\langle \delta(q_G, t) \rangle$ is the *average* thickness of the linear diffusion layer that, in general, is a function of time and of the characteristic dimensions of the electrode according to the expressions given in Table 4 for different electrode geometries. Thus, under the dkss assumptions the mathematical form of the thickness of the linear diffusion layer does not depend on the reaction mechanism considered since its expression is obtained on the basis of a "purely" diffusive problem, with the influence of the coupled chemical process(es) being included in the surface value $\zeta_s(E, \varpi, q_G, t)$.

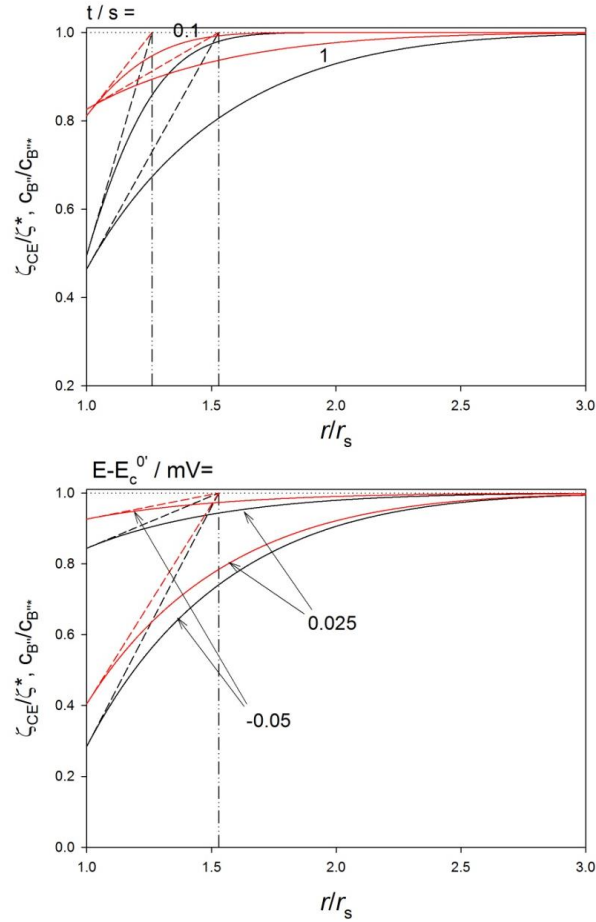


Figure 4. Dkss transient profiles of the pseudo-species ζ_{CE} / ζ^* corresponding to the CE mechanism (black line), with $\zeta_{CE} = c_B + c_C$ and $\zeta^* = c_B^* + c_C^*$, and of the species $c_{B''} / c_{B''*}$ for the EC mechanism (red line) mechanisms at a (hemi)spherical electrode calculated from Eqs. (27) and Eq. (B3) and (B4) in [17] and Eq. (A27) in [18], respectively. $\kappa = 100 \text{ s}^{-1}$, $K = 1$, $r_s = 50 \mu\text{m}$, $D = 10^{-5} \text{ cm}^2 \text{ s}^{-1}$. In Fig. 4a, $E - E^{0'} = -50 \text{ mV}$ whereas in Fig. 4b, $t = 1 \text{ s}$.

In Fig. 4 the profiles of the pseudo-species $\zeta(r, t)$ and species $c_{B''}$ corresponding to the CE and EC mechanisms, respectively, at a (hemi)spherical electrode under dkss conditions have been plotted for two values of time (Fig. 4a) and of the applied potential (Fig. 4b). These curves illustrate how within this theoretical framework the thickness of the linear diffusion layer has a transient character and its value is independent of the applied potential and of the reaction mechanism, the influence of the latter being included in the surface value of the pseudo-species ζ or species $c_{B''}$. Hence, the value of the linear diffusion layer (as well as that of the reaction layer) is defined by the shape of the electrode as shown in Figure 5 for disc and ring

microelectrodes. Note that the thickness of the linear diffusion layer $\langle \delta(q_G, t) \rangle$ is always larger than for the reaction layer and they only coincide in the catalytic mechanism (Figure 2) and in the case of very slow chemical kinetics.

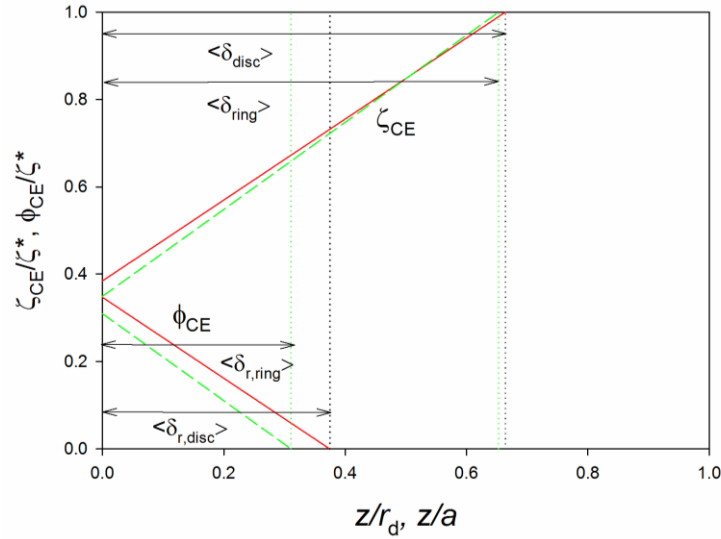


Figure 5. Dkss linear profiles of the pseudo species $\phi/\zeta^* = (\phi_s/\zeta^*)(1 - z/\langle \delta_{r,G} \rangle)$ and $\zeta/\zeta^* = (\zeta_s/\zeta^*) + (1 - (\zeta_s/\zeta^*))z/\langle \delta_G \rangle$ corresponding to the CE mechanism at a disc ($r_d = 5 \mu\text{m}$, red solid line) and a ring ($r_{r,\text{outer}} = a = 5 \mu\text{m}$ and $r_{r,\text{inner}} = 1 \mu\text{m}$, green dashed line) electrode calculated from the corresponding expressions in Tables 3 and 4 and (B3) and (B4) in [17]. $\zeta_{\text{CE}} = c_B + c_C$, $\zeta^* = c_B^* + c_C^*$ and $\phi_{\text{CE}} = c_B - Kc_C$. $\kappa = 100 \text{ s}^{-1}$, $K = 2$, $r_s = 5 \mu\text{m}$, $D = 10^{-5} \text{ cm}^2 \text{ s}^{-1}$, $E - E^0 = -100 \text{ mV}$, $t = 0.1 \text{ s}$

2.2.1. The transient current-potential response

The dkss assumptions enable the simple resolution of the diffusive-kinetic problems of all the reaction mechanisms (1)-(8) (see references [17,18,21–24] and Supporting Information for scheme (d)) and the corresponding analytical solutions has proven to yield accurate results under transient conditions for fast chemical kinetics at electrodes of any shape and size [14]. Thus, once the expressions for the linear thickness (or average linear thickness) of the diffusion and reactions layers are known for a given electrode geometry (Tables 3 and 4), the current-potential curve can be immediately calculated by applying the particular boundary conditions of each mechanism. The expressions for the current-potential response are given in Table 5 and

they enable us to study the voltammetric response for a variety of mechanisms at a wide range of microelectrode geometries.

From the expressions of the current in Table 5, an additional simplification is achieved in the limit situation where the rate constants tend to infinite, which in practice means that the thickness of the reaction layers tend to zero. This situation is referred to as "Total Equilibrium" and it implies that the chemical equilibrium is maintained at all times and points in the solution during the experiment. The simplified total equilibrium expressions, deduced from those given in Table 5 by making $\delta_{r,G} \rightarrow 0$, are given in Table 6.

2.3. Total steady-state (tss) current-potential responses

For submicroelectrodes, a total steady state behavior is attained where $\partial\phi/\partial t = \partial\zeta/\partial t = 0$. Under these conditions, both the linear diffusion layer and current response become time-independent and are only a function of the particular electrode geometry. The tss current-potential curves are easily obtained from the dkss solutions for the different reaction mechanisms by making $q_G \rightarrow 0$ in the expression of the linear diffusion layer δ_G (which will be denoted as $\delta_{ss,G}$). In the case of (hemi)spherical or hemicylindrical submicroelectrodes, the resulting expressions are exact given that the dkss assumptions are fully valid under steady state conditions. Regarding non-uniformly accessible microelectrodes, only a small intrinsic error can be expected [15] due to the assumption that ζ_s and ϕ_s take a constant value across the submicroelectrode surface (Eqs. (30) and (26), respectively), which is quite reasonable according to the results shown in Figure 6, and also to the possible empirical character of the expressions for $\delta_{r,G}$ (and δ_G).

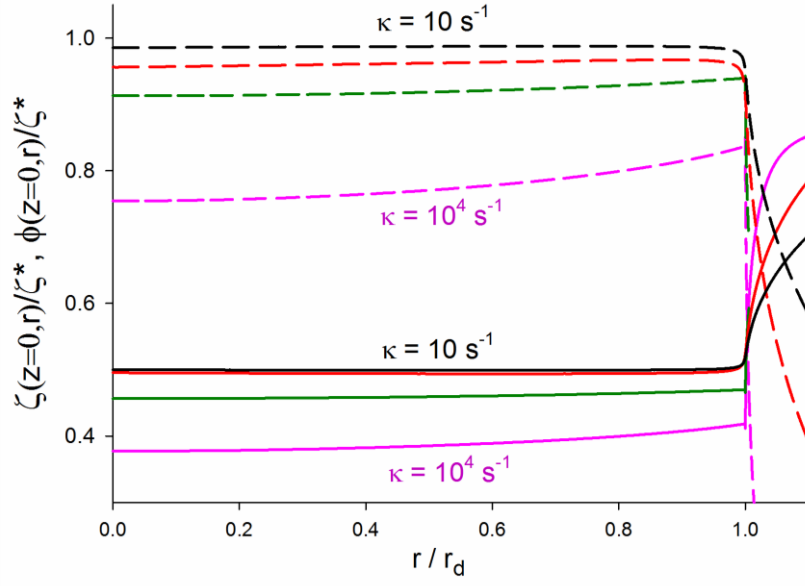


Figure 6. Surface values of the pseudo-species $\zeta = c_B + c_C$ (solid line) and $\phi = c_B - Kc_C$ (dashed line) at a disc microelectrode as a function of the distance to the electrode centre ($r = 0$) corresponding to a CE mechanism with $K = 100$ and $\kappa = 10, 10^2, 10^3, 10^4 \text{ s}^{-1}$ (from black line to pink line). $r_d = 10 \mu\text{m}$, $D = 10^{-5} \text{ cm}^2 \text{ s}^{-1}$. Curves calculated via finite-difference numerical methods [25,26]

3. Conclusions

A general solving strategy for electrochemical reaction-diffusion problems at any interface geometry has been proposed and applied to a wide variety of microelectrode geometries (hemispherical, spheroid, disc, ring, cylinder, band) and reaction mechanisms (CE, EC, ECE, CEC, square, open-square, CECEC). The theoretical approach is based on appropriate definitions of the linear reaction $\delta_{r,G}$ and diffusion δ_G layers as arising from the kinetic steady state (kss) and diffusive-kinetic steady state (dkss) approximations. The mathematical form of $\delta_{r,G}$ and δ_G is defined by the electrode geometry and it is independent of the applied potential and formally identical for any reaction mechanism. Expressions for $\delta_{r,G}$ and δ_G have been extracted for microelectrodes of very different shapes. From them, and making use of the dkss approach, closed-form equations for the transient current-potential response have been obtained that enable accurate kinetic studies with microelectrodes of typical sizes ($r_0 \leq \sqrt{Dt}$). The steady-state and the total chemical equilibrium responses can be derived as limit cases where the characteristic dimension of the electrode or the linear reaction layer tend to zero, respectively.

4. Acknowledgements

The authors greatly appreciate the financial support provided by the Fundación Séneca de la Región de Murcia (Projects 19887/GERM/15 and 18968/JLI/13) as well as by the Ministerio de Economía y Competitividad (Projects CTQ-2015-65243-P and CTQ-2015-71955-REDT Network of excellence "Sensors and Biosensors"). EL also thanks the Ministerio de Economía y Competitividad for the fellowship "Juan de la Cierva-Incorporación 2015".

Table 1. Boundary value problem corresponding to different reaction mechanisms under kinetic steady-state (kss) conditions for equal diffusion coefficients of the participating species where G refers to the electrode geometry (\equiv disc, sphere, band and cylinder). Electron transfer reactions are assumed to be reversible.

Mass transport differential equations		
Catalytic $B \xrightleftharpoons[k_2]{k_1} C + e^- \rightleftharpoons B$	CE $B \xrightleftharpoons[k_2]{k_1} C + e^- \rightleftharpoons C'$	EC $B'' + e^- \rightleftharpoons B \xrightleftharpoons[k_2]{k_1} C$
$\frac{\partial \zeta}{\partial t} = D \nabla_G^2 \zeta$ $D \nabla_G^2 \phi = \kappa \phi$	$\frac{\partial \zeta}{\partial t} = D \nabla_G^2 \zeta$ $D \nabla_G^2 \phi = \kappa \phi$ $\frac{\partial c_{C'}}{\partial t} = D \nabla_G^2 c_{C'}$	$\frac{\partial c_{B'}}{\partial t} = D \nabla_G^2 c_{B'}$ $\frac{\partial \zeta}{\partial t} = D \nabla_G^2 \zeta$ $D \nabla_G^2 \phi = \kappa \phi$
Initial and boundary conditions		
$\left. \begin{array}{l} t = 0, q \geq q_S \\ t > 0, q \rightarrow \infty \end{array} \right\}$		
$\zeta(q, t) = \zeta^*$ $\phi = 0$	$\left. \begin{array}{l} \zeta = \zeta^* \\ \phi = 0 \\ c_{C'} = 0 \end{array} \right\}$	$\left. \begin{array}{l} c_{B''} = c_{B''}^* \\ \zeta = \phi = 0 \end{array} \right\}$
$t > 0, q = q_S,$		
$\left(\frac{\partial \zeta}{\partial q_N} \right)_{q_{N,S}} = 0$	$\left(\frac{\partial \zeta}{\partial q_N} \right)_{q_{N,S}} = - \left(\frac{\partial c_{C'}}{\partial q_N} \right)_{q_{N,S}}$	$\left(\frac{\partial c_{B''}}{\partial q_N} \right)_{q_{N,S}} = - \left(\frac{\partial \zeta}{\partial q_N} \right)_{q_{N,S}}$

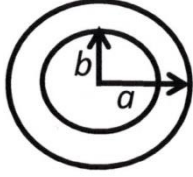
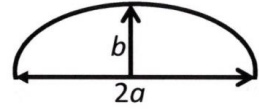
$\phi_s = \frac{1 - Ke^\eta}{1 + e^\eta} \zeta^*$	$-K \left(\frac{\partial \zeta}{\partial q_N} \right)_{q_{N,S}} = \left(\frac{\partial \phi}{\partial q_N} \right)_{q_{N,S}}$ $\zeta_s - \phi_s = (1 + K) e^\eta c_{C',s}$	$\left(\frac{\partial \phi}{\partial q_N} \right)_{q_{N,S}} = \left(\frac{\partial \zeta}{\partial q_N} \right)_{q_{N,S}}$ $c_{B'',s} (1 + K) = e^\eta (K \zeta_s + \phi_s)$
Expression of the current		
$I_{\text{cat,G}} = -FA_G D \frac{1}{1 + K} \left(\frac{\partial \phi}{\partial q_N} \right)_{q_{N,S}}$	$I_{\text{CE,G}} = FA_G D \left(\frac{\partial \zeta}{\partial q_N} \right)_{q_{N,S}}$	$I_{\text{EC,G}} = FA_G D \left(\frac{\partial c_{B''}}{\partial q_N} \right)_{q_{N,S}}$

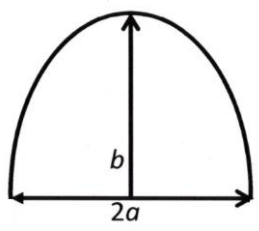
Table 2. Boundary value problem corresponding to different reaction mechanisms under kinetic steady-state (kss) conditions for equal diffusion coefficients of the participating species where G refers to the electrode geometry (\equiv disc, sphere, band and cylinder). Electron transfer reactions are assumed to be reversible.

Mass transport differential equations		
<p>CEC</p> $A'' \xrightleftharpoons[k_2]{k_1} B'' + e^- \rightleftharpoons B \xrightleftharpoons[k_2]{k_1} C$	<p>ECE</p> $B'' + e^- \rightleftharpoons B \xrightleftharpoons[k_2]{k_1} C + e^- \rightleftharpoons C'$	<p>SQ</p> $B'' + e^- \rightleftharpoons B$ $\updownarrow \qquad \updownarrow$ $C'' + e^- \rightleftharpoons C$
$\frac{\partial \zeta''}{\partial t} = D \nabla_G^2 \zeta''$ $D \nabla_G^2 \phi'' = \kappa \phi''$ $\frac{\partial \zeta}{\partial t} = D \nabla_G^2 \zeta$ $D \nabla_G^2 \phi = \kappa \phi$	$\frac{\partial c_{B'}}{\partial t} = D \nabla_G^2 c_{B'}$ $\frac{\partial \zeta}{\partial t} = D \nabla_G^2 \zeta$ $D \nabla_G^2 \phi = \kappa \phi$ $\frac{\partial c_{C'}}{\partial t} = D \nabla_G^2 c_{C'}$	$\frac{\partial \zeta''}{\partial t} = D \nabla_G^2 \zeta''$ $D \nabla_G^2 \phi'' = \kappa \phi''$ $\frac{\partial \zeta}{\partial t} = D \nabla_G^2 \zeta$ $D \nabla_G^2 \phi = \kappa \phi$
Initial and boundary conditions		
$\left. \begin{array}{l} t = 0, q \geq q_S \\ t > 0, q \rightarrow \infty \end{array} \right\}$		
$\left. \begin{array}{l} \zeta'' = \zeta^{''*} \\ \phi'' = \zeta = \phi = 0 \end{array} \right\}$	$\left. \begin{array}{l} c_{B''} = c_{B''}^* \\ \zeta = \phi = c_{C'} = 0 \end{array} \right\}$	$\left. \begin{array}{l} \zeta'' = \zeta^{''*} \\ \phi'' = \zeta = \phi = 0 \end{array} \right\}$
$t > 0, q = q_S,$		

$\left(\frac{\partial \phi''}{\partial q_N}\right)_{q_{N,S}} + K'' \left(\frac{\partial \zeta''}{\partial q_N}\right)_{q_{N,S}} = 0$ $\left(\frac{\partial \zeta}{\partial q_N}\right)_{q_{N,S}} - \left(\frac{\partial \phi}{\partial q_N}\right)_{q_{N,S}} = 0$ $\left(\frac{\partial \zeta''}{\partial q_N}\right)_{q_{N,S}} = - \left(\frac{\partial \zeta}{\partial q_N}\right)_{q_{N,S}}$ $\frac{1+K''}{1+K} e^\eta = \frac{\zeta_s'' - \phi_s''}{\phi_s + K \zeta_s}$	$\left(\frac{\partial c_{B'}}{\partial q_N}\right)_{q_{N,S}} = - \frac{1}{1+K} \left(K \left(\frac{\partial \zeta}{\partial q_N}\right)_{q_{N,S}} + \left(\frac{\partial \phi}{\partial q_N}\right)_{q_{N,S}} \right)$ $\frac{1}{1+K} \left(\left(\frac{\partial \zeta}{\partial q_N}\right)_{q_{N,S}} - \left(\frac{\partial \phi}{\partial q_N}\right)_{q_{N,S}} \right) = - \left(\frac{\partial c_{C'}}{\partial q_N}\right)_{q_{N,S}}$ $c_{B'',s} = e^{\eta_{B'/B}} \frac{\phi_s + K \zeta_s}{1+K}$ $\frac{\zeta_s - \phi_s}{1+K} = e^{\eta_{C'/C}} c_{C',s}$	$K'' \left(\frac{\partial \zeta''}{\partial q_N}\right)_{q_{N,S}} + \left(\frac{\partial \phi''}{\partial q_N}\right)_{q_{N,S}} = - \frac{1+K''}{1+K} \left(K \left(\frac{\partial \zeta}{\partial q_N}\right)_{q_{N,S}} + \left(\frac{\partial \phi}{\partial q_N}\right)_{q_{N,S}} \right)$ $\left(\frac{\partial \zeta''}{\partial q_N}\right)_{q_{N,S}} - \left(\frac{\partial \phi''}{\partial q_N}\right)_{q_{N,S}} = - \frac{1+K''}{1+K} \left(\left(\frac{\partial \zeta}{\partial q_N}\right)_{q_{N,S}} - \left(\frac{\partial \phi}{\partial q_N}\right)_{q_{N,S}} \right)$ $\zeta_s'' - \phi_s'' = e^{\eta_{C'/C}} \frac{1+K''}{1+K} (\zeta_s - \phi_s)$ $K'' \zeta_s'' + \phi_s'' = e^{\eta_{B'/B}} \frac{1+K''}{1+K} (K \zeta_s + \phi_s)$
Expression of the current		
$I_{\text{CEC,G}} = F A_G D \left(\frac{\partial \zeta''}{\partial q_N}\right)_{q_{N,S}}$	$I_{\text{ECE,G}} = F A_G D \left(2 \left(\frac{\partial c_{B'}}{\partial q_N}\right)_{q_{N,S}} + \left(\frac{\partial \zeta}{\partial q_N}\right)_{q_{N,S}} \right)$	$I_{\text{SQ,G}} = F A_G D \left(\frac{\partial \zeta''}{\partial q_N}\right)_{q_{N,S}}$

Table 3. Expression for the (average) linear thickness of the reaction layer $\langle \delta_{r,G} \rangle$ for different microelectrode geometries G (see [19] and references therein).

General expression for $\langle \delta_{r,G} \rangle$				
$\langle \delta_{r,G} \rangle = \left(\frac{4a}{A_G} \left(A_1 + B_1 \sqrt{\chi} + C_1 e^{-D_1 \sqrt{\chi}} \right) \right)^{-1}, \quad \chi = \frac{\kappa}{D} a^2$				
Electrode Geometry	A_1	B_1	C_1	D_1
Hemispherical	$\pi / 2$	$\pi / 2$	0	0
Disc	0.7854	0.7854	0.2146	0.6934
Circular Ring 	$\frac{\pi}{4} \left(1 + \frac{a}{b} \right)$	$\frac{\pi}{4} \left(1 - \left(\frac{b}{a} \right)^2 \right)$	$\left(\frac{l_0}{4a} \right) - A_1$	$\left \frac{B_1 - \frac{(l_0/a)^2}{8\pi}}{C_1} \right $
Hemi-oblate 	$\frac{\pi}{4} \left(\left(\frac{b}{a} \right) + \cos^{-1} \left(\frac{b}{a} \right) \left(1 - \left(\frac{b}{a} \right)^2 \right)^{-1/2} \right)$	$\frac{\pi}{4} \left(\left(\frac{b}{a} \right) + \cosh^{-1} \left(\frac{b}{a} \right) \left(1 - \left(\frac{b}{a} \right)^2 \right)^{-1/2} \right)$	$\left(\frac{l_0}{4a} \right) - A_1$	$\left \frac{B_1 - \frac{(l_0/a)^2}{8\pi}}{C_1} \right $

Hemi-prolate 	$\frac{\pi}{4} \left(\left(\frac{b}{a} \right) + \cosh^{-1} \left(\frac{b}{a} \right) \left(\left(\frac{b}{a} \right)^2 - 1 \right)^{-1/2} \right)$	$\frac{\pi}{4} \left(\left(\frac{b}{a} \right) + \cos^{-1} \left(\frac{b}{a} \right) \left(\left(\frac{b}{a} \right)^2 - 1 \right)^{-1/2} \right)$	$\left(\frac{l_0}{4a} \right) - A_1$	$\left \frac{B_1 - \frac{(l_0/a)^2}{8\pi}}{C_1} \right $
--	--	---	---------------------------------------	---

Pseudo steady state - $\langle \delta_{r,G} \rangle = \left(\frac{4a}{A_G} f(\chi) \right)^{-1}$, $\chi = \frac{\kappa}{D} a^2$

	$f(\chi)$ for small Values of χ	$f(\chi)$ for large Values of χ
Hemi-cylinder	$\left(\frac{2\chi}{b} \int_0^\infty \frac{e^{-\chi u}}{\ln(1.2609u)} du \right)^{-1}$	$\left(\frac{1}{b} \left(\left(\frac{b}{a} \right) \sqrt{\chi} + \frac{1}{2} \right) \right)^{-1}$
Band	$\left(\frac{2\pi\chi}{b} \int_0^\infty \frac{e^{-\chi u}}{\ln(22739.57u)} du \right)^{-1}$	$\left(\frac{1}{b} \left(\left(\frac{b}{a} \right) \sqrt{\chi} + 1 \right) \right)^{-1}$

(l_0/a) is the steady state diffusion limited current for a simple charge transfer (see [19])

Table 4. Expressions for the inverse of the thickness of the linear diffusion layers under transient ($\langle \delta_G \rangle^{-1}$) and stationary ($\langle \delta_{ss,G} \rangle^{-1}$) conditions for several electrode geometries (G=disc, sphere, band and cylinder).

Electrode	$\langle \delta_G \rangle^{-1}$	$\langle \delta_{ss,G} \rangle^{-1}$
Disc (radius r_d , Area $A_d = \pi r_d^2$)	$\frac{4}{\pi} \frac{1}{r_d} \left(0.7854 + 0.44315 \frac{r_d}{\sqrt{Dt}} + 0.2146 \exp \left(-0.39115 \frac{r_d}{\sqrt{Dt}} \right) \right)$	$\frac{4}{\pi} \frac{1}{r_d}$
Sphere (radius r_s , Area $= 4\pi r_s^2$)	$\frac{1}{r_s} + \frac{1}{\sqrt{\pi Dt}}$	$\frac{1}{r_s}$
Band (height w , length l , Area $= wl$)	$\frac{1}{w} + \frac{1}{\sqrt{\pi Dt}}$ if $Dt / w^2 < 0.4$ $0.25 \sqrt{\frac{\pi}{Dt}} e^{-0.4 \frac{\sqrt{\pi Dt}}{w}} + \frac{\pi}{w \ln \left(5.2945 + 5.9944 \frac{\sqrt{Dt}}{w} \right)}$ if $Dt / w^2 \geq 0.4$	$\frac{1}{w} \frac{2\pi}{\ln \left[64Dt / w^2 \right]}$
Cylinder (radius r_c , length l , Area $= 2\pi r_c l$)	$\frac{1}{\sqrt{\pi Dt}} e^{-0.1 \frac{\sqrt{\pi Dt}}{r_c}} + \frac{1}{r_c \ln \left(5.2945 + 1.4986 \frac{\sqrt{Dt}}{r_c} \right)}$	$\frac{1}{r_c} \frac{2}{\ln \left[4Dt / r_c^2 \right]}$

Table 5. Analytical solutions for the steady state current-potential response of the mechanisms (1)-(6) and (8) with reversible electron transfer reactions. (see [15] and references therein). The expressions for $\langle \delta_G \rangle$ and $\langle \delta_{r,G} \rangle$ are independent of the reaction mechanism and are given in Tables 3 and 4. Also note that in the SQ mechanism two linear reaction layers are defined: $\langle \delta_r \rangle$ and $\langle \delta_r' \rangle$. $\eta = F(E - E^{0'}) / RT$

Mec.	Current-potential steady state response
CE	$I_{CE} = \frac{FA_G D (c_B^* + c_C^*)}{\langle \delta_{r,G} \rangle K + \langle \delta_G \rangle (1 + (1 + K)e^\eta)}$
EC	$I_{EC} = \frac{FA_G D c_{B'}^* (1 + K)}{\langle \delta_G \rangle (1 + K) + e^\eta (\langle \delta_G \rangle K + \langle \delta_{r,G} \rangle)}$
ECE	$I_{ECE} = \frac{FA_G D c_{B'}^*}{\langle \delta_G \rangle} \frac{2 \left(\frac{K-1}{2} + \frac{\langle \delta_G \rangle}{\langle \delta_{r,G} \rangle} \right) + e^{\eta_{CC}} \frac{\langle \delta_G \rangle}{\langle \delta_{r,G} \rangle} (K+1)}{\left(1 + e^{\eta_{CC}} \right) \left(\frac{\langle \delta_G \rangle}{\langle \delta_{r,G} \rangle} + e^{\eta_{B'B}} \right) + K \left(e^{\eta_{B'B}} + 1 \right) \left(1 + \frac{\langle \delta_G \rangle}{\langle \delta_{r,G} \rangle} e^{\eta_{CC}} \right)}$
CEC	$I_{CEC} = FA_G D (c_{B'}^* + c_{C'}^*) \frac{(1 + K) / \langle \delta_{d,G}'' \rangle}{1 + K + K'' (1 + K) \frac{\langle \delta_{r,G}'' \rangle}{\langle \delta_{d,G}'' \rangle} + \left(\frac{\langle \delta_{r,G} \rangle}{\langle \delta_{d,G} \rangle} + K \right) (1 + K'') e^\eta}$
SQ	$I_{SQ} = \frac{FA_G D (c_{B'}^* + c_{C'}^*)}{\langle \delta_G \rangle} \left\{ \frac{K'' (e^{\eta_{CC}} - e^{\eta_{B'B}}) + (1 + K'') \left(\frac{\langle \delta_{r,G}'' \rangle}{\langle \delta_{r,G} \rangle} + e^{\eta_{B'B}} \right)}{(1 + K'') \left(1 + \left(\frac{1 + K''}{1 + K} \right) e^{\eta_{CC}} \right) \left(\frac{\langle \delta_{r,G}'' \rangle}{\langle \delta_{r,G} \rangle} + e^{\eta_{B'B}} \right) + \left(e^{\eta_{CC}} - e^{\eta_{B'B}} \right) \left\{ K'' + \frac{\langle \delta_{r,G}'' \rangle}{\langle \delta_G \rangle} + \left(\frac{1 + K''}{1 + K} \right) \left(K e^{\eta_{CC}} - \frac{\langle \delta_{r,G}'' \rangle}{\langle \delta_G \rangle} \right) \right\}} \right\}$
oSQ	$I_{oSQ} = \frac{FA_G D (c_{B'}^* + c_{C'}^*)}{\langle \delta_G'' \rangle} \frac{\frac{\langle \delta_G'' \rangle}{\langle \delta_{r,G}'' \rangle} (e^{\eta_{B'B}} + K e^{\eta_{CC}}) + (1 + K'') e^{\eta_{B'B}} e^{\eta_{CC}}}{e^{\eta_{CC}} \left(K'' + \frac{\langle \delta_G'' \rangle}{\langle \delta_{r,G}'' \rangle} \right) + e^{\eta_{CC}} \left(1 + K'' \frac{\langle \delta_G'' \rangle}{\langle \delta_{r,G}'' \rangle} \right) + e^{\eta_{B'B}} e^{\eta_{CC}} (1 + K'') + \frac{\langle \delta_G'' \rangle}{\langle \delta_{r,G}'' \rangle} (1 + K'')}$
Catalytic	$I_{cat} = FA_G D (c_B^* + c_C^*) \frac{1 - K e^\eta}{(1 + K)(1 + e^\eta)} \frac{1}{\langle \delta_{r,G} \rangle}$

Table 6. Expression for the total-equilibrium current of the mechanisms (1)-(5) with reversible electron transfer reactions. $\eta = F(E - E^0)/RT$

Mechanism	Current-potential response under total equilibrium
CE	$I_{\text{CE,G}} = FA_{\text{G}} D \zeta^* \frac{1}{\langle \delta_{\text{G}} \rangle} \frac{1}{1 + (1 + K) e^{\eta}}$
EC	$I_{\text{EC,G}} = FA_{\text{G}} D c_{\text{B}^*}^* \frac{1}{\langle \delta_{\text{G}} \rangle} \frac{1}{1 + \frac{K}{1 + K} e^{\eta}}$
ECE	$I_{\text{ECE,G}} = FA_{\text{G}} D c_{\text{B}^*}^* \frac{1}{\langle \delta_{\text{G}} \rangle} \frac{2 + (1 + K) e^{\eta_{\text{C/C}'}}}{1 + (1 + K) e^{\eta_{\text{C/C}'}} + K e^{\eta_{\text{B'/B}}} e^{\eta_{\text{C/C}'}}}$
CEC	$I_{\text{CEC,G}} =$ $= FA_{\text{G}} D (c_{\text{A}^*}^* + c_{\text{B}^*}^*) \frac{1}{\langle \delta_{\text{G}} \rangle} \frac{1}{1 + \frac{K(1 + K'')}{1 + K} e^{\eta}}$
SQ	$I_{\text{SQ,G}} = FA_{\text{G}} D \zeta^{''*} \frac{1}{\langle \delta_{\text{G}} \rangle} \frac{1}{1 + \frac{1 + K''}{1 + K} e^{\eta_{\text{C'/C}}}}$
Catalytic	-

References

- [1] A.J. Bard, L.R. Faulkner, *Electrochemical Methods: Fundamentals and Applications*, 2nd ed., Wiley, New York, 2000.
- [2] A. Molina, J. González, *Pulse Voltammetry in Physical Electrochemistry and Electroanalysis*, Springer International Publishing, Berlin, 2016.
- [3] R.G. Compton, C.E. Banks, *Understanding Voltammetry*, 2nd ed., Imperial College Press, London, 2010.
- [4] H.H. Girault, Charge Transfer across Liquid—Liquid Interfaces, in: Springer US, 1993: pp. 1–62.
- [5] A. Molina, E. Torralba, C. Serna, J.A. Ortuño, Analytical solution for the facilitated ion transfer at the interface between two immiscible electrolyte solutions via successive complexation reactions in any voltammetric technique: Application to square wave voltammetry and cyclic voltammetry, *Electrochim. Acta.* 106 (2013) 244–257.
- [6] I. Ruzić, S. Feldberg, The heterogeneous equivalent: A method for digital simulation of electrochemical systems with compact reaction layers, *J. Electroanal. Chem. Interfacial Electrochem.* 50 (1974) 153–162.
- [7] M. Fleischmann, F. Lasserre, J. Robinson, D. Swan, The application of microelectrodes to the study of homogeneous processes coupled to electrode reactions: Part I. EC' and CE reactions, *J. Electroanal. Chem. Interfacial Electrochem.* 177 (1984) 97–114.
- [8] K.B. Oldham, Steady-state microelectrode voltammetry as a route to homogeneous kinetics, *J. Electroanal. Chem.* 313 (1991) 3–16.
- [9] J.A. Alden, R.G. Compton, A General Method for Electrochemical Simulations. 2. Application to the Simulation of Steady-State Currents at Microdisk Electrodes: Homogeneous and Heterogeneous Kinetics, *J. Phys. Chem. B.* 101 (1997) 9606–9616.
- [10] J. Galceran, S.L. Taylor, P.N. Bartlett, Steady-state currents at inlaid and recessed microdisc electrodes for first-order EC' reactions, *J. Electroanal. Chem.* 476 (1999) 132–

147.

- [11] L. Rajendran, M. V. Sangaranarayanan, Diffusion at Ultramicro Disk Electrodes: Chronoamperometric Current for Steady-State EC' Reaction Using Scattering Analogue Techniques, *J. Phys. Chem. B.* 103 (1999) 1518–1524.
- [12] Á. Molina, I. Morales, M. López-Tenés, Chronoamperometric behaviour of a CE process with fast chemical reactions at spherical electrodes and microelectrodes. Comparison with a catalytic reaction, *Electrochem. Commun.* 8 (2006) 1062–1070.
- [13] J. Crank, *The Mathematics of Diffusion*, 2nd ed., Clarendon, Oxford, 1975.
- [14] E. Torralba, A. Molina, C. Serna, J.A. Ortuño, Rigorous Characterization of the Facilitated Ion Transfer at Ities in Normal Pulse Voltammetry. Comparison with the Approximated Treatments, *Int. J. Electrochem. Sci.* 7 (2012) 6771–6786.
- [15] Á. Molina, E. Laborda, J. González, *The reaction layer at microdiscs: A cornerstone for the analytical theoretical treatment of homogeneous chemical kinetics at non-uniformly accessible microelectrodes*, 2016.
- [16] Á. Molina, J. González, E. Laborda, M.C. Henstridge, R.G. Compton, The transient and stationary behaviour of first-order catalytic mechanisms at disc and hemisphere electrodes, *Electrochim. Acta.* 56 (2011) 7404–7410.
- [17] I. Morales, A. Molina, Analytical expressions of the I-E-t curves of a CE process with a fast chemical reaction at spherical electrodes and microelectrodes, *Electrochem. Commun.* 8 (2006) 1453–1460.
- [18] A. Molina, I. Morales, Comparison between derivative and differential pulse voltammetric curves of EC, CE and catalytic processes at spherical electrodes and microelectrodes, *Int. J. Electrochem. Sci.* 2 (2007) 386–405.
- [19] R. Senthamarai, L. Rajendran, A comparison of diffusion-limited currents at microelectrodes of various geometries for EC' reactions, *Electrochim. Acta.* 53 (2008) 3566–3578.

- [20] J.-P. Diard, B. Le Gorrec, C. Montella, Diffusion layer approximation under transient conditions, *J. Electroanal. Chem.* 584 (2005) 182–191.
- [21] A. Molina, E. Laborda, F. Martínez-Ortiz, J.M. Gómez-Gil, Normal Pulse Voltammetry and Steady State Voltammetry of the Square Mechanism at Spherical Microelectrodes, *Electroanalysis*. 27 (2015) 970–979.
- [22] A. Molina, C. Serna, J. González, General analytical solution for a catalytic mechanism in potential step techniques at hemispherical microelectrodes: Applications to chronoamperometry, cyclic staircase voltammetry and cyclic linear sweep voltammetry, *J. Electroanal. Chem.* 454 (1998) 15–31.
- [23] Á. Molina, E. Laborda, J.M. Gómez-Gil, F. Martínez-Ortiz, R.G. Compton, A Comprehensive Voltammetric Characterisation of ECE Processes, *Electrochim. Acta*. 195 (2016) 230–245.
- [24] Á. Molina, J.M. Olmos, E. Laborda, J.M. Gómez-Gil, J. González, Voltammetry of the aqueous complexation–dissociation coupled to transfer (ACDT) mechanism with charged ligands, *Phys. Chem. Chem. Phys.* 18 (2016) 17091–17104.
- [25] R.G. Compton, E. Laborda, K.R. Ward, *Understanding Voltammetry: Simulation of Electrode Processes*, Imperial College Press, London, 2014.
- [26] D. Britz, J. Strutwolf, *Digital Simulation in Electrochemistry*, Springer International Publishing, Cham, 2016.